Spatial patterns of land degradation and their impacts on the water balance of rainfed treecrops: A case study in South East Spain

van Wesemael, B.; Rambaud, X.; Poesen, J.; Muligan, M.; Cammeraat, E.; Stevens, A.

DOI
10.1016/j.geoderma.2006.03.036

Publication date
2006

Document Version
Final published version

Published in
Geoderma

Available online at www.sciencedirect.com
SCIENCE DIRECT®
GEODERMA
Geoderma 133 (2006) 43 – 56
www.elsevier.com/locate/geoderma

Spatial patterns of land degradation and their impacts on the water balance of rainfed treecrops: A case study in South East Spain

Bas van Wesemael [a,*], Xavier Rambaud [a], Jean Poesen [b], Mark Muligan [c], Erik Cammeraat [d], Antoine Stevens [a]

[a] *Geography department, Université catholique de Louvain, Place Pasteur 3, B 1348 Louvain-la-Neuve, Belgium*
[b] *Physical and Regional Geography Research Group, K.U. Leuven, Celestijnenlaan 200E, B 3001 Heverlee, Belgium*
[c] *Environmental Monitoring and Modelling Research Group, Department of Geography, King's College London, Strand, London, WC2R 2LS, United Kingdom*
[d] *Institute for Biodiversity and Ecosystem Dynamics, Universiteit van Amsterdam, Nieuwe Achtergracht 166, 1018 WV Amsterdam, The Netherlands*

Available online 19 May 2006

Abstract

Rainfed permanent crops such as almonds, olives and vines cover important areas in the drier parts of the Mediterranean. The acreage of almonds has expanded rapidly into marginal soils of the hillslopes of southeast Spain. This expansion starting in the 1970s was reinforced by the subsidies under the EU Common Agricultural Policy since the late 1980s. Trees are widely spaced and the soil in between is kept bare to reduce competition with weeds for the scarce rainfall. Hence, the large areas of bare soil are vulnerable to water erosion. However, recently it has been demonstrated that soil redistribution by tillage can be an even more important cause of degradation. This paper investigates the systematic variation in soil properties as a result of soil redistribution by tillage of a small catchment (21 ha in Murcia Region, southeast Spain) converted to almond groves in the late 1970s. Furthermore, the impacts of the spatial variation in soil properties on the water balance of the almond cropping system are evaluated. The results of a spatially distributed tillage erosion model, WATEM, are validated by a topographic survey of accumulation and removal of soil along field borders (root mean square difference (RMS) = 6.7 ton ha^{-1} y^{-1}). On the hillslopes, soil loss by tillage erosion amounts to 26.6 ton ha^{-1} y^{-1} while sedimentation occurs at a rate of 21.1 ton ha^{-1} y^{-1}. The difference between erosion and sedimentation on the hillslopes results in a net transport of sediment towards the valley bottom, where the sediment is retained behind 17 earthen dams. Overall, these currently store 156.5 tons ha^{-1}, which is about half their total capacity. The area suffering from erosion is larger (53%) than the area undergoing sedimentation (34%) or the area undergoing a change within the accuracy of the model prediction (13%). Hence, soils in a large part of the catchment become gradually thinner and stonier. The PATTERN model, developed to describe the hydrology of thin and stony soils, was validated on two columns of bare soil for which wetting and drying runs were monitored. Frequent tillage destroys the roots in the plough layer and forces the widely spaced trees to develop a lateral root system in the broken bedrock below. The model results indicate that evaporation losses (92.8–94.7 mm per year) are similar for all soil profiles regardless of landscape position. The water draining below the plough layer (i.e. 67% of the rainfall) will be used by the tree crop to develop its canopy covering the fields only partially (i.e. the transpiring surface is a fraction of the total area). However, the frequent ploughing causes important soil

* Corresponding author. Tel.: +32 10 472056; fax: +32 10 472877.
E-mail address: vanwesemael@geog.ucl.ac.be (B. van Wesemael).

doi:10.1016/j.geoderma.2006.03.036

redistribution, which reduces soil thickness on the one hand and fills up the storage behind dams in the valley bottom on the other hand.

Keywords: Soil redistribution; Tillage; Spatial variation in soil properties; Water balance; Rainfed tree crops; Southeast Spain

1. Introduction

During the last decades the acreage of rainfed tree crops such as almonds and olives has expanded rapidly in southeast Spain (Faulkner et al., 2003). Tubeileh et al. (2004) report on the recent expansion of rainfed olive groves in Syria. Mechanisation has enabled farmers to cultivate marginal soils even on steep hillslopes. The trees are widely spaced and the orchards are frequently ploughed in order to reduce competition for the scarce soil water by weeds and to increase infiltration rates. This expansion into marginal areas is stimulated by the EU Common Agricultural Policy, which directly subsidises modernisation of extensive plantations and conversion of shrubland as well as supports rural development and the agro-industry (Beaufoy, 2003). Unfortunately, the expansion of tree crops has not been accompanied by soil conservation measures and existing terraces have often even been destroyed (Oñate and Peco, 2005).

Faulkner et al. (2003) highlighted the soil degradation as a result of conversion of shrublands into almond or olive groves with widely spaced trees and hardly any plant cover. Poesen et al. (1997) quantified the soil redistribution as a result of frequent tillage and defined a diffusion constant for these marginal areas. van Wesemael et al. (2000, 2003) showed the possible impacts of soil degradation on the water balance. However, they largely worked at the hillslope scale and therefore could not quantify the spatial patterns in water availability for entire cultivated catchments.

Van Oost et al. (2000a) and De Alba (2003) have demonstrated the role of tillage in redistribution of soil within fields. Van Oost et al. (2000b) pointed to the importance of the landscape structure in producing soil loss along the upslope field border and sedimentation along the downslope border, which could reach up to 28% of the changes in annual erosion rates. These high erosion rates have been reported to result in the increase of thin and stony soils on the convexities of Mediterranean environments (Poesen et al., 1997; Kosmas et al., 2001). In particular cereals (Kosmas et al., 2001) but also vines (Ramos and Mulligan, 2005) suffer from water stress in these thin soils and clear relationships between crop yield and landscape position appear. However, such relationships between water stress and spatial patterns of soil degradation are not evident for widely spaced tree crops. These trees mine the water that penetrates through the bare soil and the tree production is maximised by adapting their spacing to the local climate (Tubeileh et al., 2004; Meerkerk and van Wesemael, 2005). Therefore, the trees do not necessarily depend on the water available in the topsoil since they extract their water from the bedrock that is ‘mouldable’ and weathers easily to produce fines. The farmers in southeast Spain state that ‘Agriculture is no longer linked to the soil, which just acts as a physical base’ (Oñate and Peco, 2005).

Research on this strategy of water harvesting is scarce since most authors concentrate on the water balance of the crop rooting in the thin soil and do not distinguish between transpiration and evaporation from the bare soil (Kosmas et al., 2001; Ramos and Mulligan, 2005). These studies do not consider evaporation from the plough layer as a loss to the amount of water percolating into the sub-soil where it can be used by the tree crop. The conversion to almond groves in the late 1970s of a small catchment on metamorphic rocks with thin soils in southeast Spain provides an excellent opportunity to study the patterns in soil properties resulting from the soil redistribution, described above, and to evaluate the effects of these patterns on the evaporation losses from the bare soils. The newly laid-out fields with access roads and a more or less even soil thickness by ripping the soil before planting are the benchmarks against which the soil redistribution models can be tested and form a starting point for the spatial patterns in soil thickness and related soil parameters.

This paper builds on previous work on soil redistribution by tillage and spatial patterns in soil properties at the scale of a small catchment (21 ha; van Wesemael et al., 2000). The paper aims to quantify the spatial variations in soil properties caused by soil degradation and their impacts on the water stress of almond trees. First, the WATEM model (Van Oost et al., 2000a) describing spatial patterns in soil redistribution will be validated. Then the PATTERN water balance model (Mulligan, 1996) will be validated for two soil profiles. The spatial pattern in soil thickness resulting from soil redistribution in a small catchment will be evaluated. Finally, the water balance for three soil profiles covering the range in soil thickness and stoniness observed will be calculated.

2. Materials and methods

2.1. Study area

The study area is located in the hills of the Sierra de Torrecilla north of La Paroquia (1°56′W, 37°41′ N, Murcia Region) in southeast Spain (Fig. 1). The Permo-Triassic slates and phyllites of the Sierra de Torrecilla represent one of the most important lithological units for rainfed agriculture in the upper Guadalentin catchment. The climate is semi arid with a mean annual precipitation of 278 mm and a mean annual temperature of 17.1 °C (Embalse de Puentes at 450 m a.s.l.). Soils are shallow grading into 'mouldable' bedrock that can easily be broken up by tillage implements. The sandy loam soils (62% sand, 32% silt and 6% clay with 1–5% organic carbon; Cammeraat and Imeson, 1998) are weakly developed Eutric Leptosols and Calcaric Regosols (ICONA, 1993) with very high rock fragment contents (66%; van Wesemael et al., 2000).

The Guadalentin catchment was one of the target areas in the MEDALUS project (Brandt and Thornes, 1996; Mairota et al., 1998). Several authors have described the study area in more detail (Boer et al., 1996; Poesen et al., 1997; Oostwoud Wijdenes et al., 1997; Cammeraat and Imeson, 1998; van Wesemael et al., 2000, 2003). The majority of the parameters in the soil redistribution and the water balance models are derived from these studies.

Within the study area a 21 ha catchment was selected belonging to a single landowner, who transformed the cereal fields into almond (*Prunus dulcis*, Miller) groves, installed or upgraded 17 check dams and created access roads along most field borders. Although the precise date of this conversion is unknown, the farmer states that it occurred in the late 1970s. In any case, the conversion is not yet visible on the 1977 aerial photos (Fig. 1).

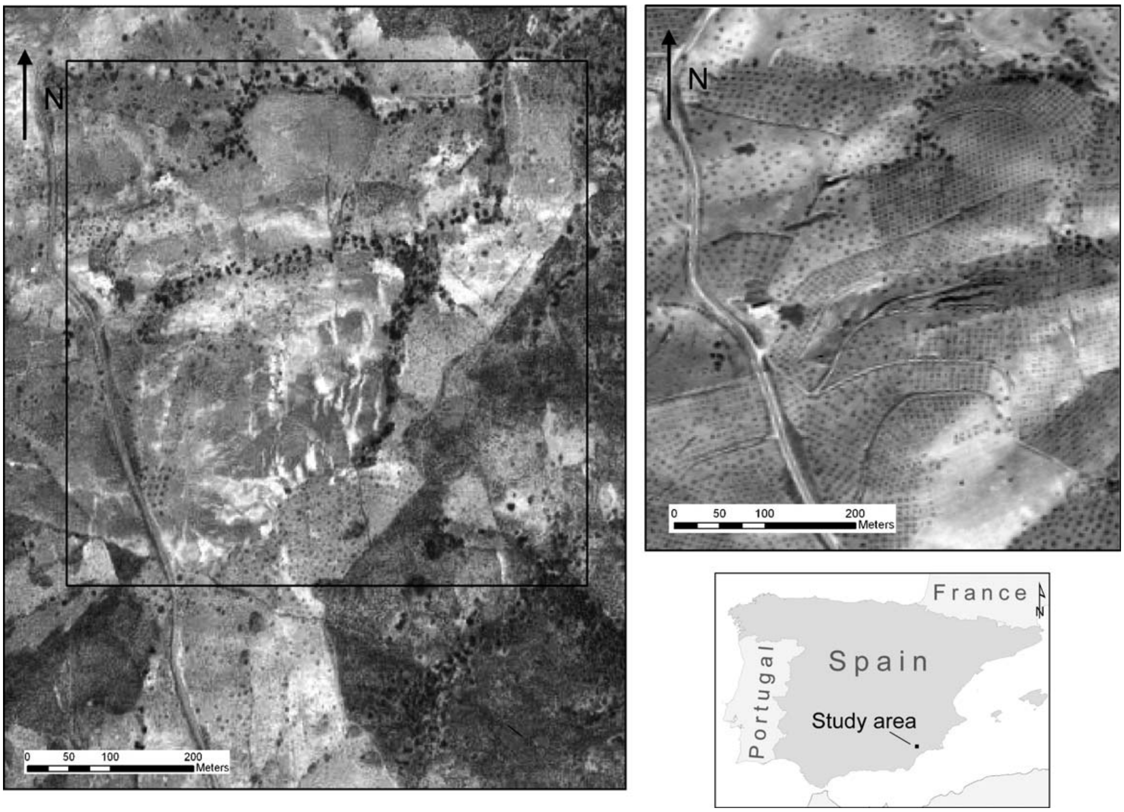

Fig. 1. Aerial photographs of the study area in 1977 (left) and 1999 (right). The almond groves and field tracks established in the late 1970s are clearly visible on the right hand photo. The DEM of Fig. 3 covers the area of the frame on the 1977 photo.

2.2. Modelling soil redistribution by tillage

Tillage erosion refers to a downslope transport of soil as a direct result of the passage with a plough (Govers et al., 1999). This transport has been described as a diffusion process for a hillslope of infinitesimal length and unit width (Eq. (1); Govers et al., 1994).

$$Q_{s,t} = k_{\mathrm{till}} \cdot \frac{\mathrm{d}h}{\mathrm{d}x} \tag{1}$$

where $Q_{s,t}$ is the net downslope flux due to tillage (kg m^{-1} y^{-1}), k_{till} is the transport coefficient (kg m^{-1}), h is the height at a given point (m) and x is the horizontal distance (m). According to Van Oost et al. (2000a) the local erosion or deposition rate (E_t in kg m^{-2} y^{-1}) can be calculated from Eq. (2):

$$E_t = \gamma \frac{\mathrm{d}h}{\mathrm{d}t} = \frac{-\mathrm{d}Q_{s,t}}{\mathrm{d}x} = -k_{\mathrm{till}} \frac{\mathrm{d}^2 h}{\mathrm{d}^2 x} \tag{2}$$

where γ is the bulk density of the soil (kg m^{-3}). Hence, tillage erosion rates depend on the change in slope gradient (Eq. (2)). In other words, soil erosion occurs on the convexities and sediment accumulation in the concavities. Furthermore, it is assumed that tillage is confined by the field boundaries and therefore these represent a line of zero flux. The WATEM model solves Eq. (2) for each grid cell of a digital elevation model (DEM; Van Oost et al., 2000a).

The DEM of the study area was constructed from a digitised topographical map of 1988 at a scale of 1:5000 with a contour interval of 5 m (Region de Murcia, 1988). A simple inverse distance interpolation was used to create a DEM with 5 m grid cells. Poesen et al. (1997) conducted a set of experiments at the same site in order to determine the k_{till}. They used four sites with different slope angles on which they retrieved tracers of different size after a passage of the tractor with a chisel plough. These experiments allowed an accurate tillage transport coefficient (k_{till}=139 kg m^{-1}) to be calculated taking into account the local implement (a chisel plough with duck feet), the dominant tillage direction (i.e. along the contours) and a tillage depth of 15 cm. The total bulk density of the stony soils was estimated at 1582 kg m^{-3} (n=20). A map with the field borders was constructed from the 1999 aerial photographs corrected by field observations. Once the input parameters are known, WATEM modifies the original DEM as a result of soil redistribution by tillage. The spatial pattern of soil redistribution is then obtained by subtracting the original DEM from the DEM created by WATEM after one model run. The soil redistribution over the entire period considered (from the late 1970s until 2000) was obtained by multiplying the results of one run by 50 (the estimated total number of tillage passes). The DEM was not corrected between tillage passes, since the soil thickness lost or gained is negligible compared to the differences in elevation between the crest and the valley bottom in this hilly catchment. The number of tillage passes between the conversion into almond fields and the validation of the model is not exactly known, but has been estimated on the basis of a minimum period (1980–2000) since conversion. When the farmer was asked to record every time he ploughed the soil, this yielded 10 tillage passes from 1994 until 1998.

2.3. Observed soil redistribution

Field borders across hillslopes (i.e. more or less parallel to the contours) are lines of zero flux for soil redistribution by tillage and therefore no soil is transported across the field border. Hence, slope discontinuities are created with an accumulation upslope and a removal downslope of the field border (Van Oost et al., 2000b). In most studies the original hillslope surface (i.e. before tillage erosion) cannot be reconstructed and therefore, no distinction between accumulation and erosion along the field border can be made (e.g. De Alba, 2003). However, most field borders in our study area consist of access roads, which allow to reconstruct the original hillslope surface (i.e. the centre of the road) and to distinguish between accumulation and removal as a result of tillage on both sides of the road (Fig. 2a). We surveyed 78 topographical transects across such field borders with a total station (i.e. a theodolite with an laser distance meter, Leica Geosystems), allowing to reconstruct 110 positive and negative lynchets (i.e. a bank formed at the end of a field by soil which, loosened by the plough, gradually moves down slope through a combination of gravity and erosion). An example of a transect through a straight slope and a convex slope with a recognisable original slope surface on the field boundary is given (Fig. 2). For the straight slopes, the cross-section of accumulated and removed soil material was calculated from the residuals of the regression through the slope profile (Fig. 2a). Convex slopes could only be used when a ridge indicating the original surface remained on the field border (Fig. 2b). The original hillslope was manually reconstructed through this ridge and the surface between the current and the original hillslope was determined by digitising the curves and calculating the surface of the polygon in AUTOCAD.

The capacity of the retention dams and the sediment behind these dams were calculated from a topographical

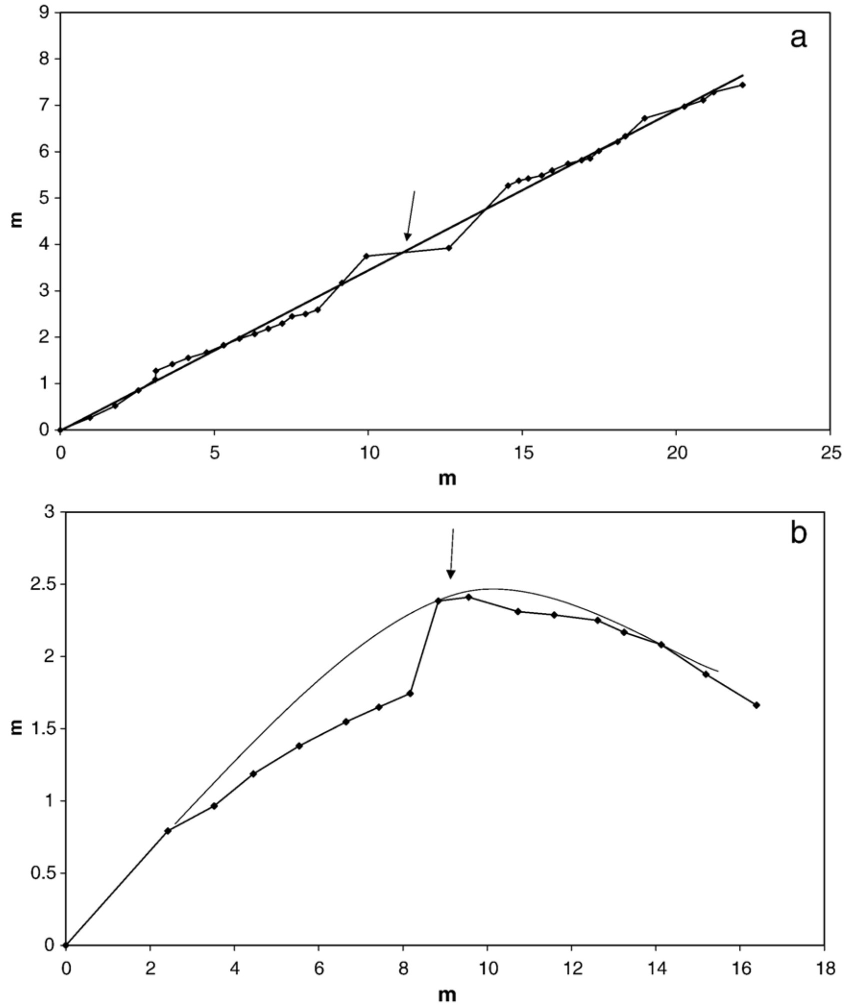

Fig. 2. Examples of transects across field borders for a straight slope (a) and a convex slope (b). The symbols are the survey points and the solid line represents the fitted original slope profile. Arrows indicate the control points used to reconstruct the original hillslope.

survey with a total station. The extremities of the top of the dam, and the sediment behind the dam were surveyed together with a long profile of the valley bottom. The capacity of the dams was represented by a prism with the apex at the intersect of a horizontal plane through the top of the dam and the long profile of the valley bottom. In case of closely spaced dams, the base of the upslope dam formed the apex of the prism representing the capacity of the dam downslope. Hence, the capacity of the dam (V in m^3) and the volume of sediment retained can be calculated from its width (W in m), distance to the intersection with the long profile (L in m) and height of the dam or the sediment behind the dam (H in m; Eq. (3)).

$$V = \frac{H \cdot L \cdot W}{6} \tag{3}$$

Studies on sediment deposits in retention ponds indicate that the error on the volumes range from 20% to 30% (Verstraeten and Poesen, 2002).

2.4. The water balance model

The PATTERN model has been developed to evaluate the hydrological effects of changes in soil properties within the context of climate variability (Mulligan, 1996). The model has been widely tested in semi-arid environments (Mulligan, 1996, 1998; van Wesemael et al., 2000; Ramos and Mulligan, 2005). The model is applied as a one-dimensional SVAT-type model at different points in the landscape. Although the model also simulates plant growth, it is applied in this study to represent the water balance of the bare soils between the widely spaced almond trees. The soil is represented in

PATTERN as a three-phase medium consisting of pore space, soil particles and organic matter and rock fragments (mineral particles > 2 mm). Water can only occupy the soil pore space. The model considers one single mixed layer.

Infiltration begins at a dry soil rate and declines towards the saturated hydraulic conductivity as soil moisture increases. The decay constant is the regression coefficient of the relation between the natural log of infiltration rate (K in mm h^{-1}) against soil moisture (K_{sat} in mm h^{-1}) based on field measurements with a double ring infiltrometer on a soil of measured porosity (so that the infiltrated water can be converted to soil moisture).

Soil evaporation is a function of the resistance to diffusion through an expanding soil surface dry layer and evaporation of ponded and canopy water also occurs, alongside transpiration. Drainage is assumed to occur at the hydraulic conductivity of the soil (K in mm h^{-1}; Eq. (4)):

$$K = K_{sat} + \left(\frac{\Theta}{\Theta_{sat}}\right) \cdot 2^{b+3} \tag{4}$$

where K_{sat} is the saturated hydraulic conductivity (mm h^{-1}), Θ is the soil moisture content and Θ_{sat} the soil moisture content at saturation (m^3 water/m^3 fine earth) and b (b-value) represents the change in matric potential per unit change in soil moisture content. Infiltration and soil evaporation are corrected for the effects of surface rock fragments and recharge is corrected for subsurface rock fragments.

The parameters required to run the PATTERN model for a bare soil are given in Table 1. Some parameters are difficult to measure directly in the skeletal soils (K, K_{sat}, decay constant, b-value and air entry value). These were estimated using the pedotransfer functions of Campbell (1985) and when necessary adjusted by a calibration.

The model runs on a variable time-step depending on the precipitation intensity. During dry periods the model runs at a day/night time-step. The meteorological inputs required are precipitation intensity, air temperature, wet bulb temperature and net solar radiation.

2.5. Calibration of the water balance model

A calibration of the daily soil moisture content predicted by the PATTERN model was carried out for two soil columns. One soil column of c. 30 cm thickness was taken on a hillslope, whereas another column of c. 50 cm thickness was sampled in a valley bottom (Table 1). The upper 10 cm of the latter soil column consists of a layer of coarse rock fragments. These profiles represent on the one hand a landscape unit suffering from soil loss (hillslope) and on the other hand a unit where accumulation occurs. The columns were transported to the laboratory and underwent four wetting and drying cycles. The soil column from the hillslope received a total precipitation of 190 mm from a rainfall simulator with an intensity of 33 mm h^{-1} and the one from the valley bottom received 200 mm. After each rainfall, they were allowed to dry for 2 to 3 months receiving radiation from UV lamps during the day at an intensity of 326.5 W m^{-2}. Radiation, air temperature and relative humidity were measured at 10 min intervals and stored in a data logger. These data were used as meteorological input to the PATTERN model at day/night time step. The soil columns were installed on an electronic balance connected to the data logger. The weight of the soil columns and the recording of the drainage by a tipping bucket raingauge allowed the calculation of the water balance (rainfall, drainage, evaporation and change in soil moisture). The accuracy of the electronic balance and the instability of the signal result in an error in the water balance of 0.4 mm for the column on the hillslope and 0.8 mm for the column from the valley bottom.

The PATTERN model was first run to simulate the evolution in soil moisture content using the K_{sat}, K, decay constant, b-value and air entry value inferred from pedotransfer functions (Table 1; Campbell, 1985). Since

Table 1
Soil properties and hydrological parameters required for the PATTERN model

	Convexity	Hillslope	Valley
Soil thickness[a] (m)	0.15	0.27	0.46
Rock fragment content by volume[b] (−)	0.47	0.40	0.53
Rock fragment cover[b] (−)	0	0	0.10
Fine earth bulk density[b] (γ_{fe} in kg m^{-3})	787	948	540
Saturated hydraulic[c] conductivity (K_{sat} in mm h^{-1})	41.9	24.1	132.6
Initial infiltration rate[c] (K in mm h^{-1})	541.9	524.1	632.6
Decay constant[d,c] (−)	−2.56	−3.08	−1.56
b-value[e,c] (−)	7.83	5.95	9.45
Air entry value[f,c] (m)	−0.052	−0.069	−0.029

[a] Estimated by the WATEM model (Fig. 5).
[b] Estimated according to the modelled spatial variation in soil depth using Eqs. (5)–(7).
[c] Estimated using the pedotransfer functions of Campbell (1985).
[d] Decay constant of the infiltration rate.
[e] b-value: change in matric potential per unit change in soil moisture (Eq. (4)).
[f] Air entry value: the matric potential at the air-entry point.

the observed soil moisture contents were not correctly reproduced, a sensitivity analysis was carried out. This analysis revealed that the *b*-value was the most critical parameter among the ones estimated by the pedotransfer functions (results not shown).

2.6. Running the water balance model taking into account the spatial variation in soil properties

Apart from the parameters determined by pedotransfer functions and adjusted by calibration (see above), the water balance model for skeletal soils requires a number of soil properties (soil thickness, rock fragment content, rock fragment cover and fine earth bulk density; Mulligan, 1996). For the marginal soils in the study area the spatial pattern of these key parameters is strongly influenced by soil redistribution. When the WATEM model runs under the assumption of an initial soil thickness and an observed average tillage depth, a spatial pattern of soil thickness due to tillage over a 25 year period will be produced. From this spatial pattern in soil thickness, the rock fragment content in the soil profile and the fine earth bulk density can be inferred (Eqs. (5) and (6)).

Stoniness increases as a result of breaking up of the bedrock by the tines of the chisel plough. Therefore, stoniness will increase with decreasing soil thickness. Soil thickness and stoniness from cultivated marginal soils were retrieved from the literature. Data for the study area were extracted from Boer et al. (1996) and van Wesemael et al. (2000) and data for marginal soils on sandstones in Greece were given in Kosmas et al. (2001). Overall, the negative linear regression between rock fragment content by mass and soil thickness was poor. However, a significant negative relationship was found between rock fragment content by mass (R_m in kg kg^{-1}) in the subsoil and soil thickness (d in m) for the study area (Eq. (5)).

$$R_m = -0.25d + 0.78 \qquad r^2 = 0.45,\ n = 31 \tag{5}$$

Finally, the fine earth bulk density (γ_{fe} in kg m^{-3}) decreases non-linearly with rock fragment content by mass (R_m in kg kg^{-1}). Torri et al. (1994) developed this relationship, which was confirmed for the study area (Eq. (6); van Wesemael et al., 2000).

$$\gamma_{fe} = 1500(1-0.85R_m^{1.93}) \qquad r^2 = 0.43,\ n = 100 \tag{6}$$

The rock fragment cover could not be directly linked to soil thickness. Apparently, the enrichment of rock fragments in the topsoil by kinetic sieving (Oostwoud Wijdenes et al., 1997), and the preferential transport of rock fragments downslope as a result of tillage (Poesen

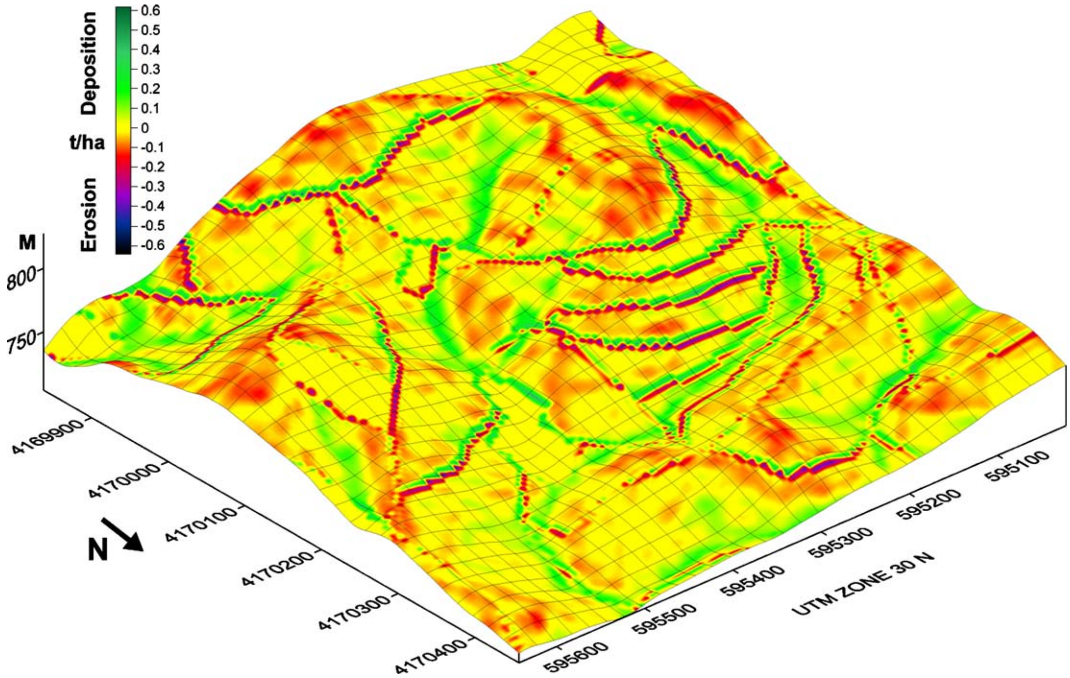

Fig. 3. Block diagram of the study area with the soil redistribution in meters after 50 tillage operations as predicted by the WATEM model. Positive values refer to sedimentation and negative values to erosion.

et al., 1997) confound this regression for the plough layer. Instead, Poesen et al. (1997) found a positive linear relationship between rock fragment cover (R_c) and hillslope curvature (C_u in % m^{-1}; convexities have positive curvature and concavities a negative curvature), although the high rock fragment cover in narrow valleys could not be explained (Eq. (7)).

$$R_c = 52.97 + 13.66C_u \qquad r^2 = 0.71,\ n = 27 \tag{7}$$

The PATTERN model was run for three soils in different landscape position i.e. convexity, straight hillslope and valley bottom using the meteorological data of an average year (1992) with 295.4 mm rainfall (Table 1; Fig. 3). Soil thickness for profiles in these positions was estimated by the WATEM model and subsequently rock fragment content, fine earth bulk density and rock fragment cover were estimated using the relationships described above (Eqs. (5)–(7); Table 1). Since the b-value was adjusted by calibration, a linear extrapolation between the values obtained for the soil columns on the hillslope and in the valley bottom was used.

3. Results and discussion

3.1. Soil redistribution by tillage

The hilly topography of the catchment (mean slope=27%) and the large number of field borders (mean parcel size=2.5 ha) result in overall high values of soil redistribution by tillage (Fig. 3). The spatial pattern of soil redistribution by tillage is well represented by the model: the convexities and upslope limits of fields lose soil, whereas the concavities and lower limits of fields gain soil. The model predicts accumulation and removal of soil along field borders to occur within a width of a single cell. This appears realistic when the size of the grid cells (5 m) is compared to the observed soil accumulation or removal across the field borders (Fig. 2). The model was validated against observed removal and accumulation along field borders for 50 tillage passes corresponding to 25 years (Fig. 4). Overall, the model predicts well with a R^2 of 0.92 and no systematic over or underestimation (regression coefficient of 1.06). The root mean square difference (RMS) between modelled and observed data is 0.0105 m, which corresponds to an error of 6.7 ton ha^{-1} y^{-1}. When we look in detail at the validation graph, an overestimation of the sediment accumulation at the downslope field borders can be observed. This overestimation can be explained by considering an interaction of tillage and water erosion. As pointed out above, the WATEM model does not consider transport between grid cells in order to calculate the erosion or accumulation (Eq. (2)). Given the fact that Govers et al. (1994) among others consider tillage erosion as a diffusion process, neglecting transport along the slope is not entirely correct. Obviously, the lack of transport is correct for erosion along the zero-flux line of the upslope field border. However, accumulation at the downslope field border is the result of transport across the entire field that stops along this line of zero flux. Apparently, not all material transported accumulates along the downslope field border (Fig. 4). This is probably due to i) the existence of concavities in the field, which are too small to be represented by the DEM, and ii) the occurrence of rills and ephemeral gullies within the fields which transport soil material directly to the valley bottom and are afterwards filled up during the subsequent tillage operation. The latter explanation is in agreement with the observation of a dense rill network after the event of September 1997 (Nachtergaele et al., 2001).

The WATEM model indicates that tillage erosion in the study area amounts to 26.6 ton ha^{-1} y^{-1} (Table 2). The intensity of soil redistribution is not only influenced by the topography but also by the landscape structure (i.e. the size and spatial pattern of the fields; Van Oost et al., 2000b). The bulk of this amount, 21.1 ton ha^{-1} y^{-1}, is retained along field borders on the hillslopes, and therefore the redistribution occurs within the fields. The difference between erosion and sedimentation on the hillslopes consists of the soil material transported by tillage erosion to the valley bottoms i.e. 5.5 ton ha^{-1} y^{-1}. These are gradually filling up, since the retention dams limit the removal of sediment from the valley bottoms by water erosion. Overall, the 17 retention dams currently store 156.5 ton ha^{-1} of sediment, which represents about half of their total capacity (318.8 ton ha^{-1}). The sediment already reaches the top of two of these dams, and their storage function is lost.

Soil thickness is determined by its initial value, the importance of losses or gains as a result of soil redistribution and the weathering rate. The minimum soil thickness will coincide with the depth of the plough layer for highly mouldable metamorphic and sedimentary rocks, since they can easily be ripped up by the tines of a chisel plough and produce enough fines to allow roots to establish. The soil redistribution discussed above has resulted in a change of soil thickness between −0.65 and +0.62 m over the 25 year period since the conversion to almond groves (Fig. 3). Spatial patterns in

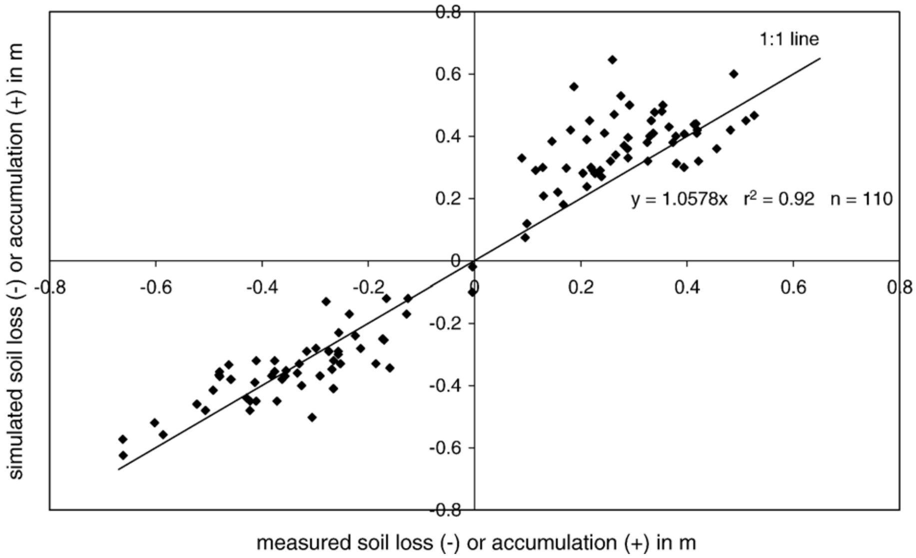

Fig. 4. Predicted versus observed soil loss (negative values) or deposition (positive values) along field borders on the hillslopes after 50 tillage operations.

weathering rates were not considered. Assuming an initial soil thickness of 30 cm (i.e. a slightly deeper soil preparation before planting) and a minimum tillage depth of 10 cm on the thinnest and stoniest soils, a distribution of soil thickness after 25 and 50 years of tillage was predicted by the WATEM model (Fig. 5). The predicted distribution of soil thickness was compared to that from 248 profile pits in the study area described by Boer et al. (1996) and van Wesemael et al. (2000). Around 90% of these soil pits were in almond groves on slates and micaschist parent material. After 25 years, the soil redistribution by tillage has not resulted in the observed variation of soil thickness, and is still too much concentrated in the class of the initial soil thickness. This could be due to an overestimation of the initial soil thickness. In the future (after 50 years of tillage), soil thickness will continue to decrease in the largest part of the catchments, except for a limited number of grid cells with a soil thickness larger than 60 cm (less than 10% of the area) where the soil thickness will further increase.

Table 2
Soil redistribution by tillage in the 21 ha catchment (see Fig. 3)

	Soil redistribution (ton ha^{-1} y^{-1})	Proportion of the catchment affected (%)
Erosion	−26.6	52.5
No change	±6.7 [a]	13.1
Sedimentation on hillslopes	+21.1	34.4
Sedimentation in valley	+5.5	34.4

[a] RMS between modelled and observed data.

The use of a single DEM (based on the 1988 topographical map), without altitude correction for erosion and sedimentation after each run, creates a possible error. Although, for some gridcells accumulation or removal can be important (−0.6 to +0.6 m; Fig. 3), the mean value for erosion over a 25 year period is limited to 42 mm. This height difference is negligible compared to the difference in altitude between two gridcells considering a mean slope gradient of 27% (i.e. 1.35 m) or the RMS of a DEM constructed from a map with a contour interval of 5 m (i.e. 1.25 m; Vandaele et al., 1996).

3.2. Impact of the spatial patterns in soil properties on the water balance

A calibration on the temporal evolution of soil moisture proved to be efficient in adjusting the b-value (Fig. 6). The RMS between measured and predicted soil moisture contents ranged from 0.0005 m^3 m^{-3} for the column in the valley bottom to 0.0009 m^3 m^{-3} for the column on the hillslope. The error in the soil moisture contents is very small (0.25 mm) and comparable to the accuracy of the tipping bucket raingauge (0.2 mm) and the electronic balances (0.4 to 0.8 mm). Still for the duration of the experiment, this results in an underestimation of the cumulative evaporation by 16% for the hillslope and 4% for the valley bottom.

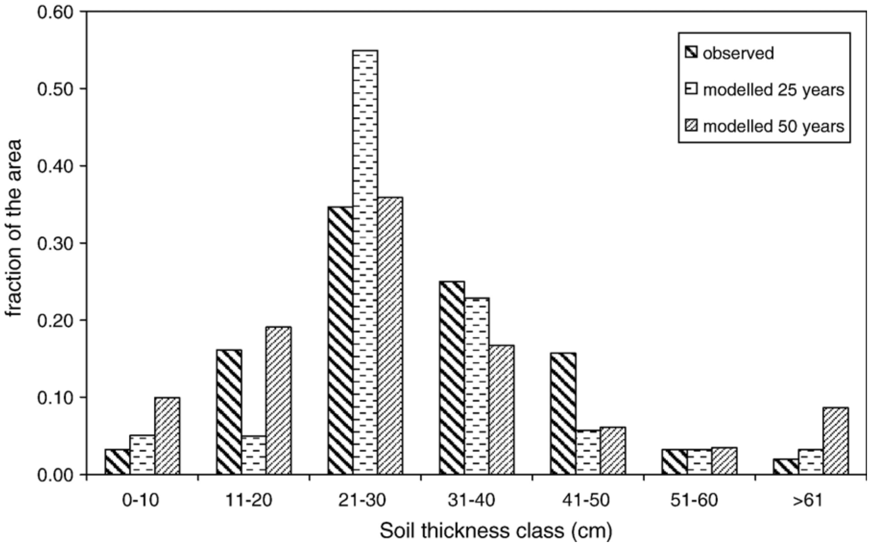

Fig. 5. Spatial distribution of soil thickness classes in the study area ($n=248$; based on Boer et al., 1996; van Wesemael et al., 2000) compared to modelled soil thickness assuming 25 and 50 years of tillage starting from a uniform soil thickness of 30 cm.

The impact of spatial patterns in soil properties on the water balance of bare soils will now be addressed. Starting from a soil moisture content of 0.15 m^3 m^{-3}, the evolution of the soil moisture content during the year 1992 shows that the moisture in the thin soils is most variable (Fig. 7). The columns reach the highest water content after rainfall and reach the lowest moisture content during summer. However, the seasonal and annual water balance of the three soil profiles does not show large differences (Table 3). Evaporation from the bare soils is almost similar for the three profiles, and so is the soil moisture depletion over the summer months. This indicates that soil moisture in the subsoil of the thicker soil column is not lost by evaporation. The stony topsoils dry out quickly and act as a barrier against evaporation (van Wesemael et al., 1996).

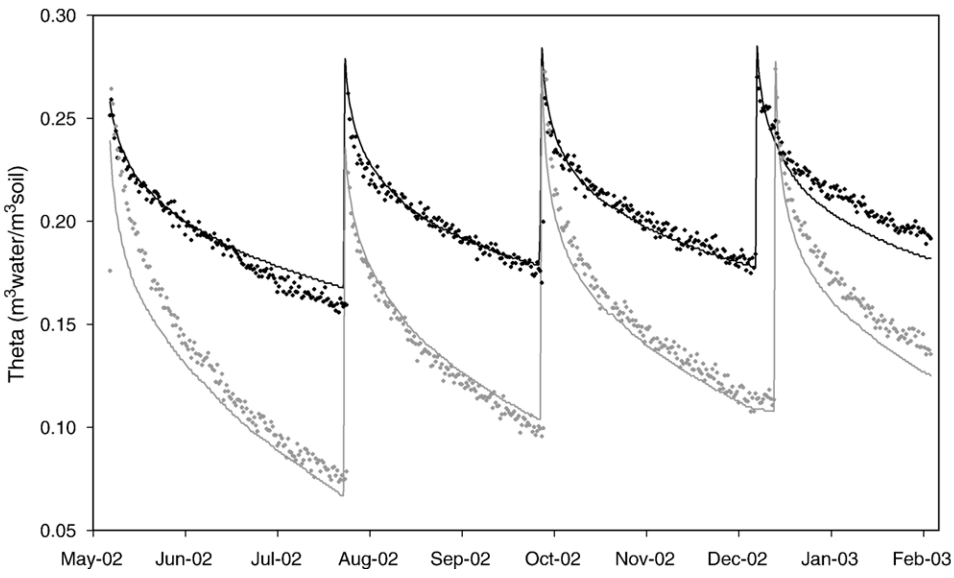

Fig. 6. Calibration of the PATTERN model. The evolution of the soil moisture content (Theta) during four wetting and drying cycles is plotted for a soil profile on the hillslope (grey symbols) and in the valley bottom (black symbols). The corresponding solid lines represent the modelled soil moisture contents.

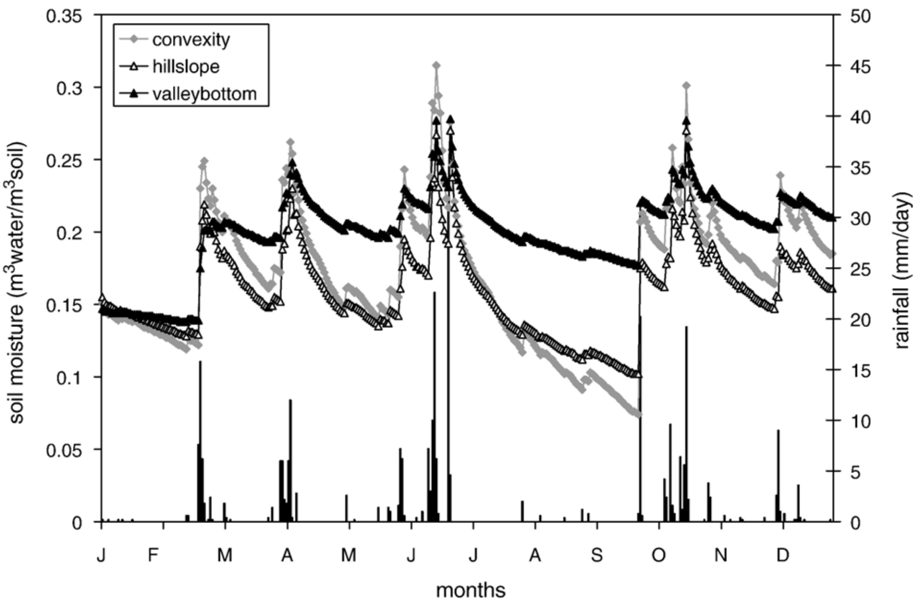

Fig. 7. Daily rainfall distribution (vertical bars) and simulated soil moisture at three landscape positions for a year with 295 mm rainfall (1992).

3.3. Rainfed almond cropping systems on marginal soils

It has been demonstrated that the clear spatial patterns in hydrological properties induced by tillage do not influence the water balance of these bare soils.

Table 3
Water balance for bare soils on the different landscape positions calculated with the PATTERN model for 1992 with an annual precipitation of 295.4 mm

	Period	Infiltration (mm)	Evaporation (mm)	Drainage (mm)	Soil moisture increment (mm)
Convexity	Annual	295.4	92.8	197.5	5.1
	DJF [a]	55.2	13.8	30.6	10.8
	MAM	64.8	27.3	34.8	2.7
	JJA	92.4	33.3	76.9	−17.8
	SON	83	18.4	55.2	9.4
Hillslope	Annual	293.6	94.7	197.3	1.6
	DJF	55.2	14.1	29.2	11.9
	MAM	64.8	27.8	36.4	0.6
	JJA	90.6	33.9	75.4	−18.7
	SON	83	18.9	56.2	7.9
Valley	Annual	295.4	94.4	172.1	28.9
	DJF	55.2	13.3	12.6	29.3
	MAM	64.8	26.6	27.7	10.5
	JJA	92.4	33.7	76.8	−18.1
	SON	83	20.8	55	7.2

[a] Seasonal water balance.

Frequent tillage eliminates the weeds and cuts the roots of the almonds forcing the trees to develop a deep rooting system. Hence, these trees are capable to mine the deeper soil layers and the joints in the soft bedrock for water. The leaf area index of the widely spaced almond trees is limited and trees can thus benefit from the water that drains through the topsoil. Since the drainage does not respond to the variability in hydrological properties of these marginal soils, a uniform cropping system can be applied.

Orgaz and Fereres (2004) argue that the canopy cover of treecrops such as almonds and olives is determined by the water availability. They propose to reduce the reference evapotranspiration (ET_0) first by a crop coefficient (k_c) and then by a reduction factor (k_r) reflecting the partial canopy cover of treecrops (Eq. (8); Allen et al., 1998; Orgaz and Fereres, 2004).

$$ET_c = ET_0 \cdot k_c \cdot k_r \qquad (8)$$

For almonds, Fereres et al. (1981) reported that a k_r of twice the fraction of the area covered by the canopy should be used. Assuming that for rainfed crops the precipitation has to supply enough moisture to meet the ET_c, the k_r and the canopy cover for the long-term average conditions can be calculated from Eq. (8). Hence, a reference evapotranspiration (ET_0 = 1068 mm), a precipitation (P = 225 mm) and a k_c of 0.65 during the growing season (March until November) result in a canopy cover of 16% (Eq. (8)). The crop water requirement data were extracted from the climate database of the Cropwat model for Murcia (Allen et al., 1998). This theoretical crop cover is lower than the canopy cover of 25% in the catchment, which was determined from the aerial photos by overlaying a grid and counting the intersects coinciding with the canopy of a tree (Fig. 1). Alternatively, the canopy cover can also be estimated by assuming that the part of the precipitation that is not lost to evaporation from bare soils ($P-E$) from the entire field can be used to support the ET_c of the canopy on a fraction of the field. In this case we do not account for the k_r in Eq. (8), but the evaporation loss is directly calculated from the PATTERN model. For 1992, the available water reaches 159 mm from March to November (Infiltration–Evaporation; Table 3). This amount of water is enough to support an ET_c of 694 mm (i.e. 0.65 * 1068) for 23% of the area. This value is much closer to the canopy cover estimated from the aerial photographs than the one derived from the empirical relations of Fereres et al. (1981). This indicates that the root systems of the almonds are efficient in using virtually all rainfall not lost to evaporation during the growing season, even when the drainage from the thin soils appears important (Table 3). Furthermore, the marginal soils with their low water holding capacity restrict evaporation losses and therefore support a higher crop density than could be expected from the study of Fereres et al. (1981) on irrigated soils.

3.4. Demonstrating the effect of landscape scale processes on crop growth

The lack of sensitivity of tree crops to spatial variation in soil properties within the catchment, demonstrated above, is in contrast with the decrease of biomass production of cereals with decreasing soil thickness (Kosmas et al., 2001). Cereals develop their root system in these marginal soils and hence depend on its water availability rather than on the drainage from the topsoils, which is the case for tree crops grown in very dry conditions. Galvez et al. (2004) demonstrated that under wetter conditions (c. 400–600 mm) olive growth is related to soil properties and also to a lesser extent to landscape position. The poor relationship with landscape position was explained by the fact that topography only indirectly influences tree growth (i.e. through soil properties and the water balance).

Although farmers are reluctant to grow cover crops, these would protect the soil from erosion and provided they develop shallow root systems, they would not compete for the water mined by the tree crops. Pastor (2004) reports experiments with cover crops in olive groves, which are ploughed under after the winter. To what extent cover crops could also be grown with an annual rainfall between 250 and 300 mm is, however, not known. Still the use of cover crops appears the way to protect marginal soils for which soil degradation is a wide spread and increasing risk in the Mediterranean basin (Beaufoy, 2003; Faulkner et al., 2003; Tubeileh et al., 2004).

4. Conclusions

Expansion of tree crop plantations in hilly areas with marginal soils can lead to significant soil redistribution by tillage (26.6 ton ha^{-1} y^{-1}). Although a large part of the soil is redistributed within the fields, a significant quantity (5.5 ton ha^{-1} y^{-1}) ends up in the valley bottom where it forms a potential source of material for water erosion. When the WATEM model is applied to a catchment that was converted to almond groves 25 years ago, distinct spatial patterns in soil thickness could be observed. Projected into the future, these patterns indicate a threat of further soil degradation and filling up of the valley bottoms. The water balance of the treecrops was represented by a two layered system: bare topsoils subjected to evaporation losses and the subsoil and soft bedrock in which the tree roots concentrate. The spatial patterns in soil properties can be quantified from the modelling of soil redistribution leading to variation in soil thickness. Soil thickness could in turn be related to rock fragment content and fine earth bulk density. However, three examples of soil profiles covering the range in variability of soil properties showed that these spatial patterns do not influence the water balance from the bare soils, and that tree crops benefit from drainage through the topsoil irrespective of the landscape position. This so-called mining for water by widely spaced tree crops is a well-known water harvesting technique throughout the Mediterranean. The low water holding capacity of stony soils reduces evaporation losses, and therefore a higher crop cover can be supported than expected from empirical relations derived from irrigated almond groves on deeper soils. Since tree growth is hardly influenced by the rapid soil degradation, farmers have no incentives to mitigate soil degradation. Further research into the possibilities to use the water in the topsoil for cover crops without compromising the water availability of the tree crops is urgently needed.

Acknowledgements

This research was carried out in the framework of the RECONDES (Conditions for Restoration and Mitigation of Desertified Areas Using Vegetation) project. RECONDES is funded by the European Commission, Directorate General of Research, Global Change and Desertification Programme, Project No. GOCE-CT-2003-505361.

References

Allen, R.G., Pereira, L.S., Raes, D., Smith, M., 1998. Crop evapotranspiration — guidelines for computing crop water requirementsFAO Irrigation and Drainage Paper 56, Rome.

Beaufoy, G., 2003. The environmental impact of olive oil production in the European Union: practical options for improving the environmental impact. European Forum on Nature Conservation and Pastoralism (73 p. http://europa.eu.int/comm/environment/agriculture/pdf/oliveoil.pdf. Last accessed in January 2006).

Boer, M., Del Barrio, G., Puigdefabregas, J., 1996. Mapping of soil depth classes in dry Mediterranean areas using terrain attributes derived from a digital elevation model. Geoderma 72, 99–118.

Brandt, J., Thornes, J.B. (Eds.), 1996. Mediterranean Desertification and Land Use. John Wiley & Sons, Chichester. 572 pp.

Cammeraat, L.H., Imeson, A.C., 1998. Deriving indicators of soil degradation from soil aggregation studies in southeastern Spain and southern France. Geomorphology 23, 307–321.

Campbell, G.S., 1985. Soil Physics with BASIC: Transport Models for Soil–Plant Systems. Department of Agronomy and Soils, Washington State University, Elsevier, New York.

De Alba, S., 2003. Simulating long-term soil redistribution generated by different patterns of mouldboard ploughing in landscapes of complex topography. Soil & Tillage Research 71, 71–86.

Faulkner, H., Alexander, R., Wilson, B.R., 2003. Changes to the dispersive characteristics of soils along an evolutionary slope sequence in the Vera badlands, southeast Spain: implications for site stabilisation. Catena 50, 243–254.

Fereres, E., Pruitt, W.O., Beutel, J.A., Henderson, D.W., Holzapfel, E., Shulbach, H., Uriu, K., 1981. ET and drip irrigation scheduling. In: Fereres, E. (Ed.), Drip Irrigation Management. Science, vol. 21259. University of California, Division of Agronomy, pp. 8–13.

Galvez, M., Parra, M.A., Navarro, C., 2004. Relating tree vigour to the soil and landscape characteristics of an olive orchard in a marly area of southern Spain. Scientia Horticulrae 101, 291–303.

Govers, G., Vandaele, K., Desmet, P.J.J., Poesen, J., Bunte, K., 1994. The role of tillage in soil redistribution on hillslopes. European Journal of Soil Science 45, 469–478.

Govers, G., Lobb, D.A., Quine, T.A., 1999. Tillage erosion and translocation: emergence of a new paradigm in soil erosion research. Soil & Tillage Research 51, 167–174.

ICONA, 1993. Proyecto LUCDEME Mapa de suelos Escala 1:100,000, Hoja 952 (Velez Blanco). Instituto Nacional para la Conservacion de la Naturaleza. Madrid.

Kosmas, C., Gerontidis, St., Marathianou, M., Detsis, B., Zafiriou, Th., van Muysen, W., Govers, G., Quine, T., Van Oost, K., 2001. The effects of tillage displaced soil on soil properties and wheat biomass. Soil & Tillage Research 58, 31–44.

Mairota, P., Thornes, J.B., Geeson, N. (Eds.), 1998. Atlas of Mediterranean desertification. The Desertification Context. Wiley, Chichester. 224 pp.

Meerkerk, A., van Wesemael, B., 2005. Plant and crop water requirements. In: Hooke, J. (Ed.), RECONDES: Conditions for Restoration and Mitigation of Desertifed Areas Using Vegetation; Review of Literature and Present Knowledge. University of Portsmouth, UK, pp. 133–139.

Mulligan, M., 1996. Modelling the complexity of land surface response to climatic variability in Mediterranean environments. In: Anderson, M.G., Brooks, S.M. (Eds.), Advances in Hillslope Processes II. Wiley and Sons, Cichester, pp. 1099–1149.

Mulligan, M., 1998. Modelling the geomorphological impact of climate variability and extreme events in a semi-arid environment. Geomorphology 24, 59–78.

Nachtergaele, J., Poesen, J., Vandekerckhove, L., Oostwoud Wijdenes, D., Roxo, M., 2001. Testing the ephemeral gully erosion model (EGEM) for two Mediterranean environments. Earth Surface Processes and Landforms 26, 17–30.

Oñate, J.J., Peco, B., 2005. Policy impact on desertification: stakeholders' perceptions in southeast Spain. Land Use Policy 22, 103–114.

Oostwoud Wijdenes, D., Poesen, J., Vandekerckhove, L., de Luna, E., 1997. Chiselling effects on the vertical distribution of rock fragments in the tilled layer of a Mediterranean soil. Soil & Tillage Research 44, 55–66.

Orgaz, F., Fereres, E., 2004. Riego, In: Barranco, D., Fernandez-Escobar, R., Rallo, L. (Eds.), El cultivo del olivo, 5th revised edition. Ediciones Mundi-Prensa, Madrid, pp. 321–346 (in Spanish).

Pastor, M., 2004. Sistemas de manejo del suelo. In: Barranco, D., Fernandez-Escobar, R., Rallo, L. (Eds.), El cultivo del olivo, 5th revised edition. Ediciones Mundi-Prensa, Madrid, pp. 229–286 (in Spanish).

Poesen, J., van Wesemael, B., Govers, G., Martinez Fernandez, J., Desmet, P., Vandaele, K., Quine, T., Degraer, G., 1997. Patterns of rock fragment cover generated by tillage erosion. Geomorphology 18, 183–197.

Ramos, M.C., Mulligan, M., 2005. Spatial modelling of the impact of climate variability on the annual soil moisture regime in a mechanized Mediterranean vineyard. Journal of Hydrology 306, 287–301.

Region de Murcia, 1988. Mapa topografico regional, escala 1:5000. Comunidad Autonoma de la Region de Murcia, Consejeria de Politica Territorial y Obras Publicas.

Torri, D., Poesen, J., Monaci, F., Busoni, E., 1994. Rock fragment content and fine soil bulk density. Catena 23, 65–71.

Tubeileh, A., Bruggeman, A., Turkelboom, F., 2004. Growing Olive Trees in Marginal Dry Environments. International Center for Agricultural Research (ICARDA), Aleppo, Syria.

Vandaele, K., Vanommeslaeghe, J., Muylaert, R., Govers, G., 1996. Monitoring soil redistribution patterns using sequential aerial photographs. Earth Surface Processes and Landforms 21, 353–364.

Van Oost, K., Govers, G., van Muysen, W., Quine, T.A., 2000a. Modelling translocation and dispersion of soil constituents by tillage on sloping land. Soil Science Society of America Journal 64, 1733–1739.

Van Oost, K., Govers, G., Desmet, P., 2000b. Evaluating the effects of changes in landscape structure on soil erosion by water and tillage. Landscape Ecology 15, 577–589.

van Wesemael, B., Cammeraat, E., Mulligan, M., Burke, S., 2003. The impact of soil properties and topography on drought vulnerability of rainfed cropping systems in southern Spain. Agriculture Ecosystems and Environment 94, 1–15.

van Wesemael, B., Mulligan, M., Poesen, J., 2000. Spatial patterns of soil water balance on intensively cultivated hillslopes in a semi-arid environment: the impact of rock fragments and soil thickness. Hydrological Processes 14, 1811–1828.

van Wesemael, B., Poesen, J., Kosmas, C.S., Danalatos, N.G., Nachtergaele, J., 1996. Evaporation from cultivated soils containing rock fragments. Journal of Hydrology 182, 65–82.

Verstraeten, G., Poesen, J., 2002. Using sediment deposits in small ponds to quantify sediment yield from small catchments: possibilities and limitations. Earth Surface Processes and Landforms 27, 1425–1439.